PERGAMON

International Journal of Heat and Mass Transfer 41 (1998) 3979–3987

International Journal of HEAT and MASS TRANSFER

Convection in a shallow rectangular cavity due to internal heat generation

P. G. Daniels*, O. K. Jones

Department of Mathematics, City University, Northampton Square, London EC1V 0HB, U.K.

Received 22 March 1996; in final form 4 February 1998

Abstract

Steady two-dimensional convective motions generated in a shallow cavity by uniformly distributed internal heat sources are analysed for the case where the vertical end walls are isothermal and the horizontal boundaries are adiabatic. Rayleigh numbers are considered for which the flow and temperature fields in the cavity are influenced by nonlinear effects. Solutions are obtained using the method of matched asymptotic expansions.

Nomenclature

c_p specific heat at constant pressure
F core stream function profile
g acceleration due to gravity
G core temperature profile
h cavity height
L cavity aspect ratio
R Rayleigh number
R_1, $\hat{R}$ scaled Rayleigh numbers
T non-dimensional temperature
$\tilde{T}$, $\hat{T}$ scaled end-region temperatures
x, z non-dimensional coordinates.

Greek symbols
β volumetric expansion coefficient
κ thermal diffusivity
ν kinematic viscosity
ξ scaled horizontal coordinate
ρ mean density
σ Prandtl number
Σ volumetric heat generation rate
ψ non-dimensional stream function
$\tilde{\psi}$, $\hat{\psi}$ scaled end-region stream functions.

1. Introduction

Motions driven by internal heat generation arise in a variety of technological applications and are of interest, for example, to the chemical and nuclear industries [1, 2] as well as in connection with related flows arising in the production of crystals by the Czochralski method [3]. There are also a variety of applications in geophysics, ranging from convection in the interior of the Earth to the motion of lakes, reservoirs and oceans and the dynamics of the atmosphere, see for example [4]. In many of these applications the flow takes place within a region of large horizontal extent and a simplified model of the physical processes can be considered to consist of a two-dimensional rectangular cavity of large aspect ratio L (width/height). Much of the previous theoretical, numerical and experimental work for such geometries [5–11] relates to cases where at least one of the horizontal surfaces is isothermal and there is an unstable stratification which at sufficiently high Rayleigh numbers supports multicellular convection.

In the present paper the steady flow produced by a uniform distribution of heat sources is studied for the case where the vertical walls are isothermal and the horizontal boundaries are adiabatic. In this case the vertical end walls of the cavity generally play a significant role. Bergholz [12] considered the high Rayleigh number limit for a cavity of finite aspect ratio, where the flow is controlled by the boundary layers on the vertical walls. A modified Oseen method of the type developed by Gill [13] was used to obtain approximate solutions. Further results for the boundary-layer regime in the large Prandtl number limit have been obtained by Blythe et al. [14] and Daniels et al. [15] using both an integral technique and a

* Corresponding author. E-mail: p.g.daniels@city.ac.uk

0017–9310/98 $19.00
PII: S0017–9310(98)00059–3

numerical solution of the vertical boundary-layer equations, and these methods have also been applied to the corresponding problem for a porous medium by Blythe et al. [16]. Experimental investigations and numerical solutions of the overall cavity flow for a range of Rayleigh numbers, Prandtl numbers and aspect ratios have been reported by Smith and Hammitt [17], Richards [18] and Kulacki and Richards [19]. Most of the experimental work relates to moderate aspect ratios, that in [17] being for $L = \frac{1}{3}$ and in [18] for $L = 1$ and $L = 2$, with Prandtl numbers in the range 4.4–7.5 and internal heating produced by ohmic resistance in the fluid. Numerical simulations reported in [18] cover aspect ratios in the range $\frac{1}{2} \leqslant L \leqslant 4$ for a Prandtl number of 6.5.

The main feature of the flow with isothermal end walls and adiabatic horizontal boundaries is a symmetric double-cell circulation with fluid ascending in the centre of the cavity and descending near the end walls. In the convection-dominated boundary-layer regime referred to above, the core flow is vertically stratified, whereas for sufficiently low Rayleigh numbers it can be expected that lateral conduction will dominate, leading to a horizontal stratification. As the Rayleigh number increases, nonlinear convective effects become important and modify this stratification, leading to a family of different flow patterns and temperature fields. For shallow cavities this family can be determined analytically. The problem is formulated in Section 2 and the critical range of Rayleigh numbers is identified, leading to an asymptotic expansion of the solution which is presented in Section 3. This expansion is found to be valid throughout most of the cavity (or core region) but near the vertical end walls must be replaced by local expansions which describe the turning motion there. These end regions are considered in Section 4 and the local solution of the nonlinear governing equations, which draws on previous results for laterally heated cavities [20] leads to the completion of the core solution to the second level of approximation. The main properties of the thermal and flow fields in the core are described in Section 5 and the results are discussed in Section 6.

2. Formulation

For steady, two-dimensional motion subject to the Oberbeck–Boussinesq approximation, the vorticity and energy equations can be written in dimensionless form as

$$\nabla^4\psi = \sigma^{-1}\frac{\partial(\nabla^2\psi,\psi)}{\partial(x,z)} + R\frac{\partial T}{\partial x} \tag{2.1}$$

$$\nabla^2 T + 1 = \frac{\partial(T,\psi)}{\partial(x,z)}. \tag{2.2}$$

Here

$$\sigma = \nu/\kappa \tag{2.3}$$

is the Prandtl number of the fluid, where ν is the kinematic viscosity and κ is the thermal diffusivity and

$$R = \frac{g\beta\Sigma h^5}{\rho c_p \nu\kappa^2} \tag{2.4}$$

is the Rayleigh number based on the cavity height h, the constant volumetric heat generation rate Σ, the acceleration due to gravity g, the volumetric expansion coefficient β, the mean density ρ and the specific heat at constant pressure c_p. In (2.1) and (2.2) the coordinates (x, z), stream function ψ and temperature T are nondimensionalized with respect to h, κ and $h^2\Sigma/\rho c_p\kappa$, respectively.

The boundary conditions at the rigid horizontal surfaces are

$$\psi = \frac{\partial\psi}{\partial z} = \frac{\partial T}{\partial z} = 0 \quad \text{on } z = \pm\frac{1}{2} \tag{2.5}$$

and at the vertical end walls

$$\psi = \frac{\partial\psi}{\partial x} = T = 0 \quad \text{on } x = 0, L \tag{2.6}$$

where L is the aspect ratio of the cavity, which is assumed to be large.

It can be expected that solutions of (2.1), (2.2), (2.5) and (2.6) exist satisfying the symmetry relations

$$\psi(x,z) = -\psi(L-x,z), \quad T(x,z) = T(L-x,z). \tag{2.7}$$

For sufficiently small Rayleigh numbers, the temperature field is dominated by conduction associated with the left-hand side of the energy equation (2.2), and the relevant solution which satisfies the thermal boundary conditions is

$$T = \tfrac{1}{2}x(L-x). \tag{2.8}$$

It is of interest to consider how large the Rayleigh number must be for this quadratic form to be modified by the effects of convection. The flow generated in the cavity by the buoyancy term in (2.1) has a stream function of order RL and from (2.2) this in turn generates a vertical temperature variation of order RL^2. Integration of (2.2) and use of the boundary conditions at $z = -\frac{1}{2}$ and $z = \frac{1}{2}$ gives

$$\int_{-1/2}^{1/2}\frac{\partial^2 T}{\partial x^2}\mathrm{d}z + 1 = -\int_{-1/2}^{1/2}\frac{\partial}{\partial x}\left(\psi\frac{\partial T}{\partial z}\right)\mathrm{d}z \tag{2.9}$$

and from the above argument it follows that the right-hand side is of order R^2L^2. Thus, the result (2.8) will no longer hold when R is of order L^{-1} and the present work is concerned with a description of flows for which the scaled Rayleigh number

$$R_1 = RL \tag{2.10}$$

is of order one as $L \to \infty$.

3. Core region

Throughout most of the cavity the solution depends on length scales

$$\xi = x/L, \quad z = z \tag{3.1}$$

and the stream function and temperature fields can be expanded in the form

$$\psi = \psi_0(\xi, z) + L^{-1}\psi_1(\xi, z) + L^{-2}\psi_2(\xi, z) + \cdots \tag{3.2}$$

$$T = L^2 T_0(\xi, z) + LT_1(\xi, z) + T_2(\xi, z) + L^{-1}T_3(\xi, z) + \cdots \tag{3.3}$$

as $L \to \infty$. These forms are now substituted into the governing equations (2.1), (2.2) and boundary conditions (2.5) to obtain a succession of problems as follows. From (2.2) at order L^2,

$$\frac{\partial^2 T_0}{\partial z^2} = 0 \tag{3.4}$$

and the solution satisfying the adiabatic conditions $\partial T_0/\partial z = 0$ at $z = \pm\frac{1}{2}$ is

$$T_0 = \theta_0(\xi) \tag{3.5}$$

where θ_0 is an arbitrary function of ξ. From (2.1) at order one,

$$\frac{\partial^4 \psi_0}{\partial z^4} = R_1 \frac{\partial T_0}{\partial \xi} \tag{3.6}$$

and the solution for ψ_0 satisfying the boundary conditions $\psi_0 = \partial\psi_0/\partial z = 0$ at $z = \pm\frac{1}{2}$ is

$$\psi_0 = R_1 \theta_0' F(z) \tag{3.7}$$

where

$$F(z) = \frac{1}{24}\left(\frac{1}{4} - z^2\right)^2. \tag{3.8}$$

From (2.2) at order L,

$$\frac{\partial^2 T_1}{\partial z^2} = \frac{\partial T_0}{\partial \xi}\frac{\partial \psi_0}{\partial z} \tag{3.9}$$

and the solution satisfying the conditions $\partial T_1/\partial z = 0$ at $z = \pm\frac{1}{2}$ is

$$T_1 = R_1 \theta_0' G(z) + \theta_1(\xi) \tag{3.10}$$

where it is convenient to choose the form of G which is an odd function of z, so that

$$G(z) = \frac{1}{24}\left(\frac{z^5}{5} - \frac{z^3}{6} + \frac{z}{16}\right) \tag{3.11}$$

and θ_1 is an arbitrary function of ξ. From (2.1) at order L^{-1},

$$\frac{\partial^4 \psi_1}{\partial z^4} = \frac{1}{\sigma}\left(\frac{\partial^3 \psi_0}{\partial z^2 \partial \xi}\frac{\partial \psi_0}{\partial z} - \frac{\partial^3 \psi_0}{\partial z^3}\frac{\partial \psi_0}{\partial \xi}\right) + R_1 \frac{\partial T_1}{\partial \xi} \tag{3.12}$$

and the solution which satisfies the conditions $\psi_1 = \partial\psi_1/\partial z = 0$ at $z = \pm\frac{1}{2}$ is

$$\psi_1 = R_1^2 \theta_0' \theta_0''(G_1(z) + \sigma^{-1}F_1(z)) + R_1 \theta_1' F(z) \tag{3.13}$$

where G_1 and F_1 are odd functions of z defined by

$$G_1 = \frac{1}{72}\left\{\frac{z^9}{2520} - \frac{z^7}{840} + \frac{z^5}{320} - \frac{11z^3}{8064} + \frac{z}{6144}\right\} \tag{3.14}$$

$$F_1 = \frac{1}{3456}\left\{\frac{z^9}{21} - \frac{z^7}{35} - \frac{z^5}{40} + \frac{5z^3}{336} - \frac{17z}{8960}\right\}. \tag{3.15}$$

From (2.2) at order one,

$$\frac{\partial^2 T_2}{\partial z^2} = -1 - \frac{\partial^2 T_0}{\partial \xi^2} + \frac{\partial T_1}{\partial \xi}\frac{\partial \psi_0}{\partial z} + \frac{\partial T_0}{\partial \xi}\frac{\partial \psi_1}{\partial z} - \frac{\partial T_1}{\partial z}\frac{\partial \psi_0}{\partial \xi}. \tag{3.16}$$

Integration in z and use of the boundary conditions $\partial T_2/\partial z = 0$ at $z = \pm\frac{1}{2}$ shows that this equation has a consistent solution only if θ_0 satisfies the equation

$$\theta_0'' + aR_1^2 \theta_0'^2 \theta_0'' + 1 = 0 \tag{3.17}$$

where

$$a = 3\int_{-1/2}^{1/2} F^2 \, \mathrm{d}z = 1/120960. \tag{3.18}$$

The second term in (3.17) represents the effect of convection on the core temperature field which must now be found by solving the nonlinear equation (3.17) subject to the end conditions

$$\theta_0 = 0 \quad \text{at } \xi = 0, 1. \tag{3.19}$$

These conditions are needed to ensure that the thermal boundary conditions on the end walls of the cavity are satisfied; the solution near the ends is considered separately in Section 4 below. Once θ_0 is found from (3.17) and (3.19), the leading order core flow field is determined from (3.7). Solutions for θ_0 are described in Section 5.

The core solution is now continued one stage further in order to determine the unknown function $\theta_1(\xi)$ which arises in the solution for T_1. The solution of (3.16) for T_2 can be expressed in the form

$$T_2 = -\frac{1}{2}z^2(1 + \theta_0'') + R_1^2 \theta_0'^2 \theta_0'' \int_0^z \int_0^z (2GF' - F^2)\, \mathrm{d}z\, \mathrm{d}z + \theta_0' \int_0^z \psi_1 \, \mathrm{d}z + \theta_1' \int_0^z \psi_0 \, \mathrm{d}z + \theta_2(\xi) \tag{3.20}$$

where θ_2 is an arbitrary function of ξ. An expression for $\partial^2 T_3/\partial z^2$ can be obtained from terms of order L^{-1} in (2.2) and integration in z and use of the boundary conditions $\partial T_3/\partial z = 0$ and $\psi_2 = 0$ at $z = \pm\frac{1}{2}$ yields

$$\int_{-1/2}^{1/2} \frac{\partial^2 T_1}{\partial \xi^2}\mathrm{d}z = \int_{-1/2}^{1/2} \left\{\frac{\partial T_2}{\partial \xi}\frac{\partial \psi_0}{\partial z} + \frac{\partial T_1}{\partial \xi}\frac{\partial \psi_1}{\partial z} - \frac{\partial T_2}{\partial z}\frac{\partial \psi_0}{\partial \xi} - \frac{\partial T_1}{\partial z}\frac{\partial \psi_1}{\partial \xi}\right\}\mathrm{d}z. \tag{3.21}$$

Contributions to these integrals arise only from those

parts of the integrands which are even in z, leading to the result

$$\theta_1'' = -aR_1^2\theta_0'(2\theta_0''\theta_1' + \theta_0'\theta_1''). \tag{3.22}$$

This equation can be integrated once to obtain

$$\theta_1' = a_1(1+aR_1^2\theta_0'^2)^{-1} \tag{3.23}$$

where a_1 is a constant of integration, but the symmetry relations (2.7) imply that $a_1 = 0$. Hence

$$\theta_1 = C \tag{3.24}$$

where C is a constant.

In summary, the core solution has been obtained in the form

$$\left.\begin{aligned} T &= L^2\theta_0(\xi) + L\{R_1\theta_0'^2G(z) + C\} + O(1) \\ \psi &= R_1\theta_0'F(z) + L^{-1}\{R_1^2\theta_0'\theta_0''(G_1(z) + \sigma^{-1}F_1(z))\} \\ &\qquad + O(L^{-2}) \end{aligned}\right\} \tag{3.25}$$

as $L \to \infty$, where C is a constant to be determined. Since it cannot be expected that θ_0' vanishes at $\xi = 0$ and $\xi = 1$, it is clear that the solution (3.25) does not satisfy the boundary conditions (2.6) on the end walls of the cavity. The necessary adjustment occurs in roughly square end regions which accommodate the turning motion of the fluid and serve to determine the value of C. These are considered next.

4. End regions

Because of the symmetry properties (2.7) it is only necessary to consider the solution near one end of the cavity. It is envisaged that $\theta_0'(0) > 0$ so that as $\xi \to 0$, the core solution (3.25) has the form

$$T \sim L^2b\xi + L\{R_1b^2G(z) + C\}, \quad \psi \sim R_1bF(z) \tag{4.1}$$

where $b = \theta_0'(0)$. This suggests that in the end region near $x = 0$ where x and z are of order one, the solution can be expanded in the form

$$T = L\tilde{T}(x,z) + \cdots, \quad \psi = \tilde{\psi}(x,z) + \cdots \tag{4.2}$$

as $L \to \infty$. Substitution into (2.1) and (2.2) shows that $\tilde{T}$ and $\tilde{\psi}$ satisfy the equations

$$\nabla^4\tilde{\psi} = \frac{1}{\sigma}\frac{\partial(\nabla^2\tilde{\psi},\tilde{\psi})}{\partial(x,z)} + R_1\frac{\partial\tilde{T}}{\partial x} \tag{4.3}$$

$$\nabla^2\tilde{T} = \frac{\partial(\tilde{T},\tilde{\psi})}{\partial(x,z)} \tag{4.4}$$

and from (2.5) and (2.6) it is required that

$$\tilde{\psi} = \frac{\partial\tilde{\psi}}{\partial z} = \frac{\partial\tilde{T}}{\partial z} = 0 \quad \text{on } z = \pm\frac{1}{2} \tag{4.5}$$

and

$$\tilde{\psi} = \frac{\partial\tilde{\psi}}{\partial x} = \tilde{T} = 0 \quad \text{on } x = 0. \tag{4.6}$$

In addition the solution must match with that given by (4.1) as $x \to \infty$, requiring that

$$\tilde{T} \sim bx + R_1b^2G(z) + c, \quad \tilde{\psi} \sim R_1bF(z), \quad x \to \infty \tag{4.7}$$

where $C = c$. It should be noted that (4.3) and (4.4) constitute the full nonlinear Boussinesq system except that the heat source term is too small to contribute, the flow being driven by the thermal gradient and recirculating flow set up in the core. In fact the parameter b can be replaced by unity in the system (4.3)–(4.7) through the scale transformations

$$\tilde{T} = b\hat{T}(x,z), \quad \tilde{\psi} = \hat{\psi}(x,z), \quad R_1 = \hat{R}b^{-1} \tag{4.8}$$

in which case the system for $\hat{\psi}$, $\hat{T}$, $\hat{R}$ is identical to that which arises in the end zone of a laterally heated cavity, for which

$$\hat{T} \sim x + \hat{R}G(z) + \hat{c}, \quad x \to \infty \tag{4.9}$$

and numerical solutions have been obtained using a finite difference method by Wang and Daniels [20]. Values of the parameter $\hat{c} = \hat{c}(\hat{R},\sigma)$ have been obtained for $\sigma = 0.71$ and a wide range of values of $\hat{R}$, and the streamline and isotherm patterns reported there are directly relevant to the present problem through the transformations (4.8). In particular, the constant C in the core solution (4.1) is determined as

$$C = b\hat{c}(bR_1,\sigma). \tag{4.10}$$

The form of $\hat{c}$ has been found by Cormack et al. [21] in the limit as $\hat{R} \to 0$ through a combination of analytical and numerical techniques, the flow in the end zone in this limit being equivalent to a Stokes flow driven by the uniform gradient $\hat{T} = x$. The core solution has the property that $b = \theta_0'(0) \to \frac{1}{2}$ as $R_1 \to 0$ (to be confirmed below) in which case their results carry over to the present problem and it follows from (4.10) that

$$C \sim 2.2\times10^{-7}R_1^2, \quad R_1 \to 0 \tag{4.11}$$

for general values of σ. In general, the parameter b is a function of R_1 which must be found by solving the core problem (3.17), (3.19); this is undertaken next.

5. Core solution

Equation (3.17) can be integrated once and the symmetry of the solution used to obtain

$$\theta_0' = a^{-1/2}R_1^{-1}(F^+(\xi) + F^-(\xi)) \tag{5.1}$$

where

$$F^\pm(\xi) = \{\tfrac{3}{2}a^{1/2}R_1(\tfrac{1}{2} - \xi) \pm (1 + \tfrac{9}{4}aR_1^2(\xi - \tfrac{1}{2})^2)^{1/2}\}^{1/3}. \tag{5.2}$$

One further integration making use of the substitution

$$y = \sinh^{-1}(\tfrac{3}{2}a^{1/2}R_1(\xi - \tfrac{1}{2})) \tag{5.3}$$

and the boundary conditions (3.19) gives the core temperature field

$$\theta_0 = a^{-1}R_1^{-2}(\cosh\tfrac{2}{3}y - \tfrac{1}{2}\cosh\tfrac{4}{3}y - \cosh\tfrac{2}{3}y_0 + \tfrac{1}{2}\cosh\tfrac{4}{3}y_0) \tag{5.4}$$

where $y_0 = \sinh^{-1}(\frac{3}{4}a^{1/2}R_1)$. From (3.7) the core stream function is given by

$$\psi_0 = -2a^{-1/2}F(z)\sinh\tfrac{1}{3}y \tag{5.5}$$

and the vertical velocity in the core is

$$w_0(\xi, z) = -\partial\psi_0/\partial\xi = \frac{R_1F(z)}{1+aR_1^2\theta_0'^2} = \frac{R_1F(z)}{1+4\sinh^2\frac{1}{3}y}. \tag{5.6}$$

Note that at the centre of the cavity, where $\theta_0' = 0$, w_0 is an exact linear function of R_1, being given by $w_0(\frac{1}{2}, 0) = R_1/384$. Profiles of θ_0, ψ_0 and w_0 are shown in Figs 1–3, and Fig. 4 summarizes the variation of the main properties of the solution with R_1.

At small values of R_1 the solution is dominated by conduction, with

$$\left.\begin{aligned}\theta_0 &\sim \tfrac{1}{2}\xi(1-\xi) + \tfrac{1}{12}aR_1^2\{(\xi-\tfrac{1}{2})^4 - \tfrac{1}{16}\} + \cdots\\ \psi_0 &\sim \{R_1(\tfrac{1}{2}-\xi) + \tfrac{1}{3}aR_1^3(\xi-\tfrac{1}{2})^3 + \cdots\}F(z)\end{aligned}\right\}(R_1 \to 0) \tag{5.7}$$

while for large values of R_1 the main balance is between convection and the internal heat source, with

$$\left.\begin{aligned}\theta_0 &\sim 3^{4/3}a^{-1/3}R_1^{-2/3}\tfrac{1}{4}\{(\tfrac{1}{2})^{4/3} - (\xi-\tfrac{1}{2})^{4/3}\}\\ \psi_0 &\sim 3^{1/3}a^{-1/3}R_1^{1/3}(\tfrac{1}{2}-\xi)^{1/3}F(z)\end{aligned}\right\}(R_1 \to \infty) \tag{5.8}$$

for $0 < |\xi - \frac{1}{2}| \leqslant \frac{1}{2}$. These forms are singular as $\xi \to \frac{1}{2}\pm$ and near the centre of the cavity there is a local smoothing of the solution on an inner length scale $\xi - \frac{1}{2} = O(R_1^{-1})$ where conduction remains significant. Here $y = O(1)$ and the full versions of the expressions (5.4) and (5.5) determine the variation of the order R_1^{-2} and order one components of the local temperature and stream function fields, respectively.

6. Discussion

A self-consistent asymptotic description of the steady-state flow generated in a shallow two-dimensional cavity by uniform internal heating has been obtained for Rayleigh numbers R of order L^{-1}. It has been shown that in this range the flow and temperature fields in the cavity are influenced by convective effects leading to changes in the shape and speed of the main double-cell circulation. Figure 5 shows the core streamlines obtained from (5.5) for various values of $R_1 = RL$. At small values of R_1 the flow is dominated by conduction and the speed of the upward motion in the double cell is virtually independent

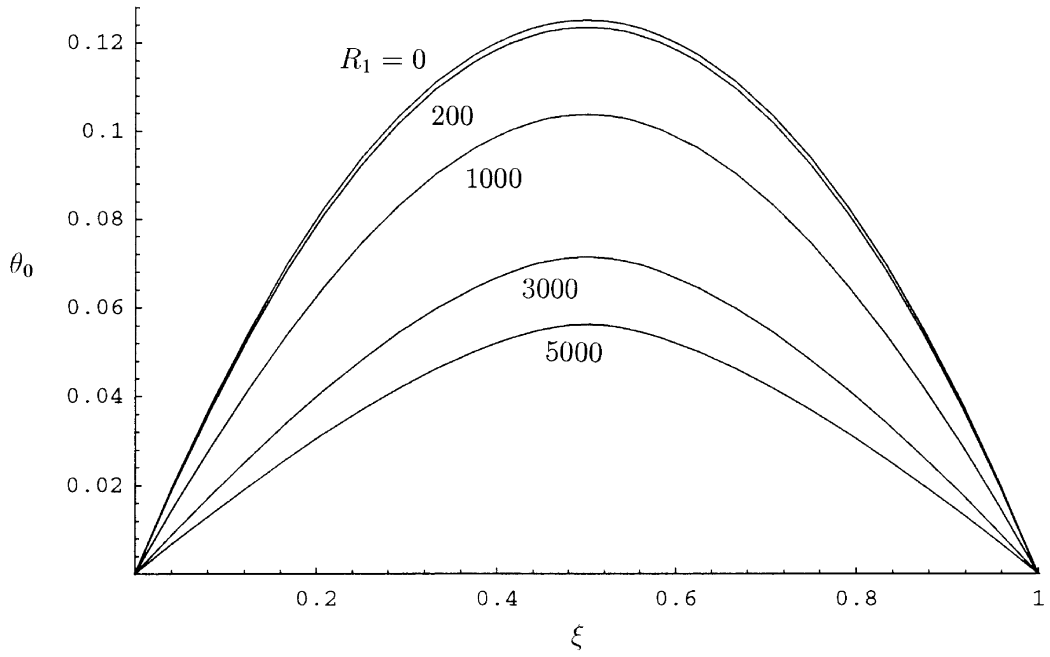

Fig. 1. Profiles of the core temperature field θ_0 for various values of R_1.

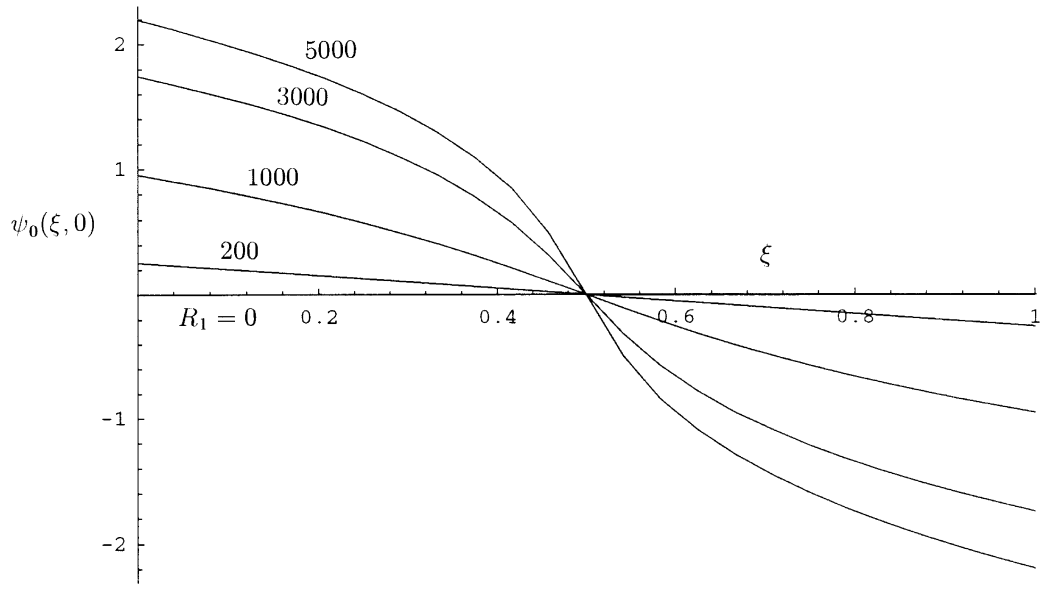

Fig. 2. Profiles of the core stream function field ψ_0 at mid-cavity height, $z = 0$, for various values of R_1.

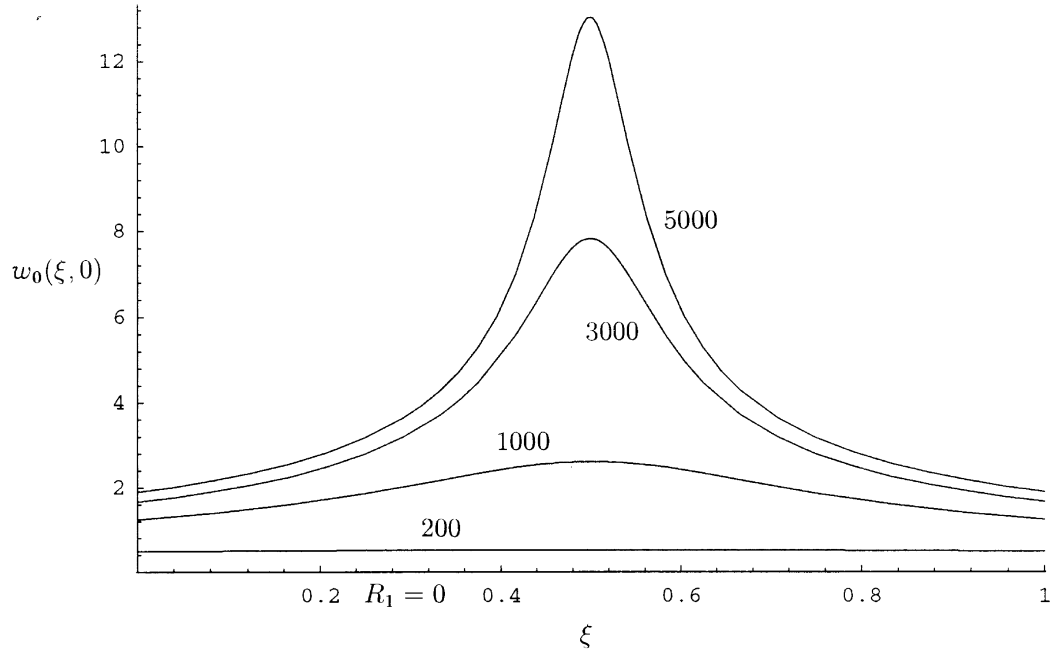

Fig. 3. Profiles of the core vertical velocity w_0 at mid-cavity height, $z = 0$, for various values of R_1.

of the lateral direction. Only near the ends of the cavity is there a significant change, and the two circulations are completed by downward motion within the end regions identified in Section 4. As R_1 increases and convection becomes more important the upward motion in the double cell becomes significantly stronger towards the centre of the cavity (Fig. 3), remaining relatively weak near the two ends. Eventually the motion at the centre leads to a new local structure there, when R is of order one. At this point the inner region identified at the end of Section 5 has width comparable to the height of the cavity and the local order one variations in ψ

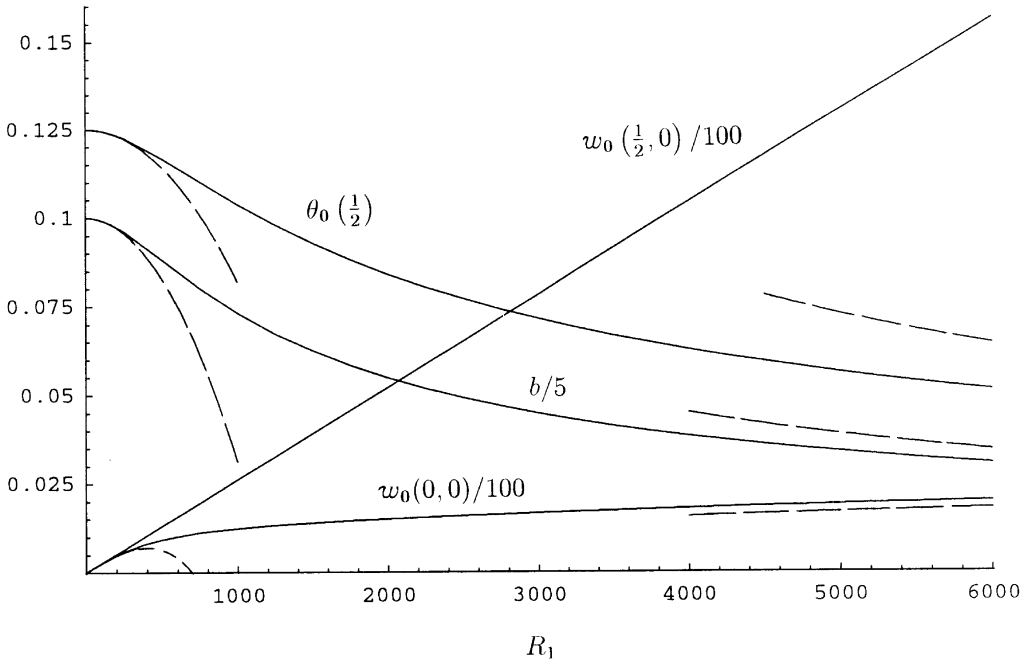

Fig. 4. Variation of the main properties of the core solution with R_1, showing (a) the temperature θ_0 at $\xi = \frac{1}{2}$, (b) the temperature gradient $b = \mathrm{d}\theta_0/\mathrm{d}\xi$ at $\xi = 0$, (c) the vertical velocity w_0 at $\xi = 0$, $z = 0$ and (d) the vertical velocity w_0 at $\xi = \frac{1}{2}$, $z = 0$. Asymptotic results obtained from (5.7) and (5.8) are shown by broken lines.

and T [relative to the constant temperature $\frac{1}{4}(\frac{3}{5})^{4/3}a^{-1/3}R^{-2/3}L^{4/3}$ implied by (5.8)] are governed by the full nonlinear system (2.1), (2.2). A proper treatment of the mathematical problem associated with this central plume will require a significant numerical investigation, which it is hoped to pursue in the near future.

In contrast, the end region flows relevant in the present regime where $R_1 = O(1)$ have already received significant attention and are nonlinear throughout the range $0 < \hat{R} < \infty$ studied by Wang and Daniels [20]. Here R_1 and $\hat{R}$ are related by $R_1 = \hat{R}/b$, with the parameter b determined from the core solution (5.1) as

$$b = \theta_0'(0) = 2a^{-1/2}R_1^{-1}\sinh\tfrac{1}{3}y_0 \tag{6.1}$$

and shown as a function of R_1 in Fig. 4. Since

$$\left.\begin{aligned} &b \to \tfrac{1}{2}, \quad R_1 \to 0 \\ &b \sim (\tfrac{3}{2})^{1/3}a^{-1/3}R_1^{-2/3}, \quad R_1 \to \infty \end{aligned}\right\} \tag{6.2}$$

it follows that

$$\left.\begin{aligned} &R_1 \sim 2\hat{R}, \quad \hat{R} \to 0 \\ &R_1 \sim \tfrac{2}{3}a\hat{R}^3, \quad \hat{R} \to \infty \end{aligned}\right\} \tag{6.3}$$

so that the family of end-region flows relevant here over the range $0 < R_1 < \infty$ correspond to the full range of solutions $0 < \hat{R} < \infty$ studied in [20]. These turning flows become quite complicated at high values of $\hat{R}$, with the formation of thin layers around the side and bottom walls and a complex eddy structure in the lower corner. At small Prandtl numbers and sufficiently high Rayleigh numbers the end-zone flow is also subject to multiple-cell instability of the type first analysed by Hart [22, 23] in the context of laterally heated cavities. Similar instabilities can therefore be expected to arise in the present internally-heated flow although it is not clear to what extent any instability will prevail throughout the cavity, given that away from the ends the core flow here is significantly different from the parallel flow of the laterally heated case. It is hoped to investigate the stability properties of the internally-heated system in future work, and it is also hoped to extend the present analysis to the case of a stress-free upper surface, of relevance in geophysical applications. The present approach is also applicable in the case of a porous medium and a parallel investigation of that problem is reported elsewhere [24].

Heat transfer properties of the system should also be mentioned. An average Nusselt number for the system based on the heat transfer through the end wall at $x = 0$ relative to the maximum temperature difference in the cavity (measured by the temperature at $x = \frac{1}{2}L, z = \frac{1}{2}$) can be defined as

$$Nu = \frac{1}{T(\frac{1}{2}L,\frac{1}{2})}\int_{-1/2}^{1/2}\frac{\partial T}{\partial x}(0,z)\,\mathrm{d}z. \tag{6.4}$$

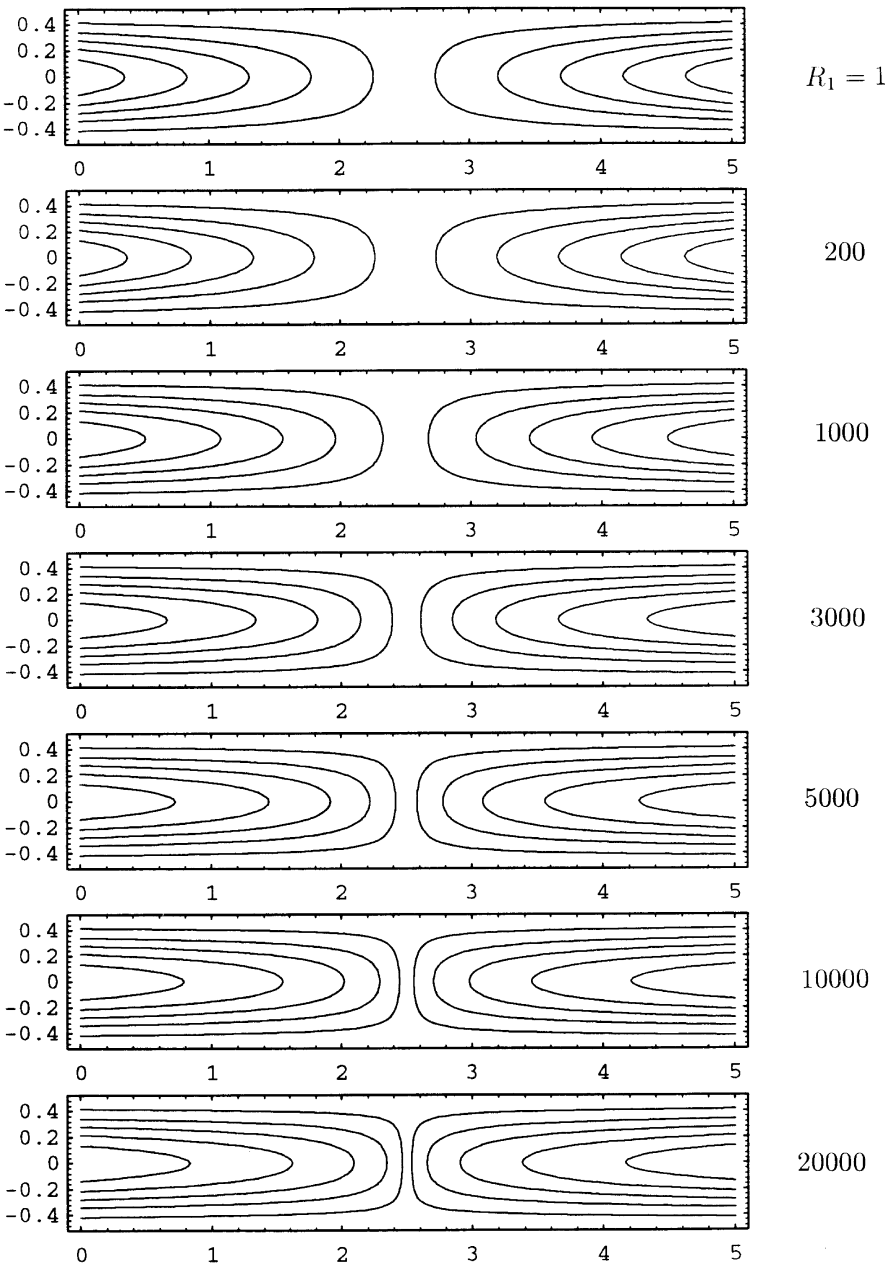

Fig. 5. Core streamlines obtained from (5.5) for various values of R_1 and shown for the case where the aspect ratio $L = 5$.

However, it follows from integration of (2.9) with respect to x and use of the symmetry properties of the flow that

$$\int_{-1/2}^{1/2} \frac{\partial T}{\partial x}(0,z)\,\mathrm{d}z = x + \int_{-1/2}^{1/2} \left(\frac{\partial T}{\partial x} - T\frac{\partial \psi}{\partial z}\right)\mathrm{d}z = \frac{1}{2}L. \tag{6.5}$$

This result expresses the fact that the total heat transfer through each end wall is precisely half that produced by the internal heat sources distributed over the total area L of the cavity. It can readily be confirmed that for the core solution (3.2), (3.3) the central expression in (6.5) is indeed constant and equal to $\frac{1}{2}L$, to the level of approxi-

mation calculated in Section 3. It follows from (6.5) that for order one values of R_1,

$$Nu = L/\{2T(\tfrac{1}{2}L,\tfrac{1}{2})\} \sim 1/\{2L\theta_0(\tfrac{1}{2})\}, \quad L \to \infty \tag{6.6}$$

where $\theta_0(\frac{1}{2})$ is sketched as a function of R_1 in Fig. 4. Of course the local distribution of heat transfer along the end wall must be obtained from the solution of the end region problem of Section 4. The results given for a range of Rayleigh numbers and several different Prandtl numbers in [20] show that most of the outward transfer of heat occurs through the upper half of the end wall where the relatively high temperature of the fluid arriving from the centre of the cavity must undergo a rapid adjustment.

The present theory is valid for large aspect ratios, $L \gg 1$, and formally speaking, for Rayleigh numbers $R_1 \ll L$. In practice the central plume mentioned earlier will emerge on a lateral scale $x \sim 1$, comparable with the height of the cavity, when from (5.3), $R_1 \sim \frac{2}{3}a^{-1/2}L \approx 232L$. This gives a rough indication of the upper limit of validity of the present theory, for the region near the centre of the cavity. A comparison with the experimental observations reported in [17] and [18] is not appropriate because the aspect ratios considered there are no larger than 2. However, a numerical simulation reported in [18] for $L = 4$, $\sigma = 6.5$ and a Rayleigh number equivalent here to $R_1 = 781.25$ should be in reasonable agreement and, indeed, the value of the Nusselt number found there, $Nu \approx 1.05$, is within 8% of the value 1.14 predicted by (6.6). The next correction to the asymptotic result (6.6) implied by (3.25), $-\frac{1}{2}L^{-2}C/\{\theta_0(\frac{1}{2})\}^2$, is of the right sign to produce even closer agreement. It is hoped that further experimental and numerical work will eventually allow a more detailed comparison with the present theory.

Acknowledgement

The authors are grateful to Mr N. Antoine for assistance in production of the figures using Mathematica.

References

[1] Gabor JD, Baker Jr. L, Cassulo JC, Mansoori, GA. Heat transfer from heat-generating boiling pools. AIChE Symp Series 1978;73:78.
[2] Baker Jr. L, Faw RE, Kulacki FA. Post-accident heat removal. I. Heat transfer within an internally heated, non-boiling liquid layer. Nucl Sci Eng 1976;61:222.
[3] Miller DC, Pernell TL. Fluid flow patterns in a simulated garnet melt. J Crystal Growth 1982;57:253.
[4] Pedlosky J. Geophysical Fluid Dynamics. Springer Verlag, N.Y., 1979.
[5] Tritton DJ, Zarraga MN. Convection in horizontal layers with internal heat generation. Experiments. J Fluid Mech 1967;30:21.
[6] Roberts PH. Convection in horizontal layers with internal heat generation. Theory. J Fluid Mech 1967;30:33.
[7] Thirlby R. Convection in an internally heated layer. J Fluid Mech 1970;44:673.
[8] Kulacki FA, Goldstein RJ. Thermal convection in a horizontal fluid layer with uniform volumetric energy sources. J Fluid Mech 1972;55:271.
[9] Kulacki FA, Emara AA. Steady and transient thermal convection in a fluid layer with uniform volumetric energy sources. J Fluid Mech 1977;83:375.
[10] Emara AA, Kulacki FA. A numerical investigation of thermal convection in a heat-generating fluid layer. ASME J Heat Transfer 1980;102:531.
[11] Churbanov AG, Vabishchevich PN, Chudanov VV, Strizhov VF. A numerical study of natural convection of a heat-generating fluid in rectangular enclosures. Int J Heat Mass Transfer 1994;37:2969.
[12] Bergholz RF. Natural convection of a heat generating fluid in a closed cavity. ASME J Heat Transfer 1980;102:242.
[13] Gill AE. The boundary layer regime for convection in a rectangular cavity. J Fluid Mech 1966;26:515.
[14] Blythe PA, Daniels PG, Simpkins PG. Convection in a rectangular cavity due to internal heat generation. AT&T Bell Lab Tech Mem 1983 (unpublished).
[15] Daniels PG, Blythe PA, Simpkins PG. The vertical boundary layer flow generated by internal heating in a rectangular cavity. AT&T Bell Lab Tech Mem 1984 (unpublished).
[16] Blythe PA, Daniels PG, Simpkins PG. Convection in a fluid-saturated porous medium due to internal heat generation. Int Comm Heat Mass Transfer 1985;12:493.
[17] Smith WL, Hammitt FG. Natural convection in a rectangular cavity with internal heat generation. Nucl Sci Eng 1966;25:328.
[18] Richards DE. Thermal convection with internal heating in vertical rectangular cavities. PhD dissertation, Ohio State University, 1981.
[19] Kulacki FA, Richards DE. Proc NATO Adv Study Inst: Natural Convection: Fundamentals and Applications, Cesme, Turkey, 1984.
[20] Wang P, Daniels PG. Numerical solutions for the flow near the end of a shallow laterally heated cavity. J Eng Math 1994;28:211.
[21] Cormack DE, Leal LG, Imberger J. Natural convection in a shallow cavity with differentially heated end walls. Part 1. Asymptotic theory. J Fluid Mech 1974;65:209.
[22] Hart JE. Stability of thin non-rotating Hadley circulations. J Atmos Sci 1972;29:687.
[23] Hart JE. Low Prandtl number convection between differentially heated end walls. Int J Heat Mass Transfer 1983;26:1069.
[24] Mohamed RA. Some problems of flow of viscous fluids in a porous medium. PhD dissertation, Qena, Egypt: South Valley University, 1995.